JAAS
Journal of Analytical Atomic Spectrometry

Accepted Manuscript

This article can be cited before page numbers have been issued, to do this please use: Ž. Zacharauskas, P. E. Warwick, B. C. Russell, D. Reading and I. W. Croudace, *J. Anal. At. Spectrom.*, 2023, DOI: 10.1039/D3JA00045A.

View Article Online
DOI: 10.1039/D3JA00045A

Development of an Optimised Method for Measurement of Iodine-129 in Decommissioning Wastes Using ICP-MS/MS

Žilvinas Zacharauskas[1,2], Phil Warwick[1,3], Ben Russell[2], Dave Reading[3], Ian Croudace[1]

[1] *School of Ocean and Earth Science, National Oceanography Centre, University of Southampton, Southampton, SO14 3ZH*

[2]*Nuclear Metrology Group, National Physical Laboratory, Hampton Rd, Teddington, TW11 0LW, United Kingdom*

[3]*GAU Radioanalytical, National Oceanography Centre, University of Southampton, Southampton, SO14 3ZH*

Abstract

Accurate, low-level measurement of the long-lived fission product ^{129}I is important for waste characterisation and long-term monitoring of waste facilities and the surrounding environment. Inductively coupled plasma mass spectrometry (ICP-MS) is well-suited to high throughput, sensitive measurement of ^{129}I as a cost-effective alternative to other mass spectrometric and decay counting techniques. Accurate ^{129}I measurement by ICP-MS is affected by the multiple interferences on m/z = 129, necessitating multi-stage sample preparation and/or mathematical correction. This study assesses the capabilities of tandem ICP-MS/MS for rapid and routine measurement of ^{129}I in nuclear wastes. The advantages of the tandem setup for removal of isobaric, polyatomic and tailing interferences are demonstrated, as are the improvements in sensitivity through matrix modification and the importance of selecting an appropriate internal standard. The optimised setup was applied to measurement of various decommissioning waste simulants following direct extraction of ^{129}I. The procedure achieved an instrument detection limit of 1.05×10^{-4} Bq g^{-1} (0.017 ng g^{-1}) for ^{129}I, which is two orders of magnitude below the target out-of-scope limit of 0.01 Bq g^{-1} (1.57 ng g^{-1}), with good agreement between ICP-MS/MS and liquid scintillation counting (LSC). The results show that rapid, routine, low-level measurement of ^{129}I is achievable by ICP-MS/MS for end users in decommissioning and environmental monitoring.

1. Introduction

The decommissioning of nuclear reactor and reprocessing facilities represents a major global challenge to the nuclear industry. Estimated costs range from £99 billion to £232 billion over the next 120 years in the UK alone[1]. Nuclear decommissioning and waste repository risk assessment must be underpinned by reliable, accurate characterisation to ensure assignment to the appropriate waste stream, which is achieved through the development of robust, reproducible and efficient radioanalytical procedures for a range of radionuclides in varied and complex sample matrices.

One radionuclide of interest is the long-lived fission product ^{129}I (half-life $16.1(7)\times10^6$ years), which is produced by thermal neutron induced fission of ^{235}U (0.706 % yield), spontaneous fission of ^{238}U, and neutron activation of ^{128}Te[2]. Iodine-129 is also produced naturally by cosmic-ray spallation of Xe isotopes in the atmosphere. Iodine-129 decays to ^{129}Xe via β-decay with a decay energy of 151.2 keV and associated gamma emission at 39.58 keV (7.42 %) and multiple X-ray emissions.

The high mobility and volatility of ^{129}I means it can migrate away from nuclear fuel via several mechanisms. In advanced gas-cooled reactors (AGRs) iodine is transported in the gaseous phase, following the release of elemental iodine from CsI particles formed within nuclear fuel[2,3,4,5,6,7]. Gaseous ^{129}I is deposited in reactor construction materials and graphite moderators surrounding the reactor and in activated carbon cooling gas filters. In light water reactors (LWRs), metal iodides are dissolved and transported around the cooling water circuit and are subsequently removed by ion exchange resin beds. Aqueous iodide can also partition into the gas phase as either elemental iodine or through conversion to an organic iodide such as CH_3I via reaction with organic impurities in paints and surface coatings.

Mechanisms including filters and ion exchangers are used to treat various reactor liquids and to retain iodine in reprocessing plants[8]. The filter materials used can include high purity cellulose and powdered anion and cation exchange resins, activated charcoal, as well as zeolite materials such as clinoptilolite, which are used as part of effluent treatment strategy to remove $^{134/137}Cs$ and ^{90}Sr at nuclear reprocessing sites[9]. In the UK, cooling ponds and reprocessing facilities also produce a $Mg(OH)_2$ sludge or slurry and silo liquors from corroding Magnox fuel and cladding rich in Mg-Al alloy that the ^{129}I may be incorporated into, which will ultimately require characterisation prior to waste sentencing.

Robust and reproducible characterisation of waste materials is essential for correct sentencing to the appropriate waste stream, involving reliable assessment of activity concentrations against waste acceptance criteria. Free release of waste requires confirmation that ^{129}I activities are below the out-of-scope limit of 0.01 Bq g^{-1} (1.57 ng g^{-1})[10]. This has been achieved in previous studies focused on environmental matrices including water, soil, plants, milk and in ambient air as particulate and gaseous ^{129}I[11,12,13,14,15,16,17], with relatively limited measurement of decommissioning wastes.

Iodine-129 has been routinely measured radiometrically using liquid scintillation counting (LSC) or gross beta measurement following isolation of ^{129}I as well as via radiochemical neutron activation analysis (RNAA)[2,18,19]. Low energy gamma spectrometry has been used to quantify ^{129}I via measurement of the 39.58 keV gamma photopeak (7.42% yield) and associated X-ray emissions[2,11,21,22]. However, this is relatively insensitive with chemical separation often still required to overcome significant Compton backgrounds at low energy arising from other fission products present at higher activity concentrations and is therefore only applied to higher activity measurements.

The long half-life and correspondingly low specific activity (6.37×10^6 Bq/g) make ^{129}I well suited to measurement by mass spectrometry (Table 1). Accelerator mass spectrometry (AMS) has been the most sensitive technique applied to date, with measurement of $^{129}I/^{127}I$ ratios in the 10^{-13}-10^{-10} range[2,12,16,17,20,21,22,23,24]. Limitations to AMS for routine nuclear waste characterisation are the relatively high cost, limited availability and analytical flexibility.

Table 1. Comparison of techniques for ^{129}I analysis

Detection method	Sample matrix	Detection Limit	$^{129}I/^{127}I$ ratio	Reference
X-ray and γ spectrometry	Tissue Urine Plant material Radioactive waste	100-200 mBq 20 mBq	10^{-4}-10^{-5} 10^{-5}-10^{-6}	2,11,20,21
LSC	Soil Plant material Water Effluent Filter	10 mBq	10^{-5}-10^{-6}	2,18,19
RNAA	Soil Sediment Plant material Tissue Water samples	1 µBq	10^{-6}-10^{-10}	21,23,25
AMS	Soil Soil leachate Plant material Thyroid tissue Water samples	10^{-3}µBq	10^{-10}-10^{-13}	12,20,21,23,24
ICP-MS	Water	10 - 100 µBq mL^{-1}	10^{-5}-10^{-6}	21,26,27,28
	Soil Sediments Water Plant material Radioactive waste	2.5 µBq g^{-1}	10^{-7}	2,21,27
ICP-MS/MS	Water Soil	0.1 µBq g^{-1}	10^{-6}-10^{-8}	13,14,15

Although ICP-MS cannot match the sensitivity of AMS, it is a widely available and flexible analytical technique that has been applied to measurement of a range of radionuclides in decommissioning wastes, including ^{129}I[26,27,29,30,31,32,33]. The volatility of Iodine in acidic conditions means it is typically introduced into the ICP-MS in dilute alkaline solution, such as NaOH, NH_4OH or tetramethyl ammonium hydroxide (TMAH)[34,35,36]. Measurement sensitivity for ^{129}I is low relative to most elements due to a high first ionisation energy of 10.45 eV[21,37,38]. Improvements in sensitivity have previously been investigated for difficult-to-ionise elements, including B, Se, I and Hg, using various carbon modifiers[39]. The carbon rich modifier allows a charge transfer reaction to occur from argon (first

DOI: 10.1039/D3JA00045A

ionisation energy 15.76 eV) to carbon species (first ionisation energy 11.26 eV) in the plasma, with further charge transfers to the difficult-to-ionise elements, increasing the signal sensitivity.

Accurate measurement of ^{129}I by ICP-MS is complicated by isobaric interferences from ^{129}Xe (26.40% abundance) present as an impurity in the argon plasma gas, multiple plasma and reaction cell-derived polyatomic interferences including $^{127}I^{1}H_2$, $^{97}Mo^{16}O_2$, $^{113}Cd^{16}O$, $^{115}In^{14}N$ and $^{89}Y^{40}Ar$, and tailing from high concentrations of stable ^{127}I (100% abundance), which cannot be chemically separated[15,27,28,30,31,40]. Isobaric ^{129}Xe has been corrected by monitoring ^{131}Xe (4.07% abundance) and using the known $^{129}Xe/^{131}Xe$ isotopic ratio[26,27,31], or suppressing the signal using a combination of collision and reaction gases (He and O_2)[21,28], at the expense of reduced analyte sensitivity[2]. Polyatomic interferences can be removed using offline chemical separation and/or collision/reaction cell ICP-MS. The extent of ^{127}I tailing removal required depends on the nature of the sample. Decommissioning samples typically have $^{129}I/^{127}I$ ratios on the order of 10^{-3}-10^{-6}, which is within range of the abundance sensitivity of ICP-MS instruments. By comparison, ratios as low as 10^{-13} may be required for pre-nuclear environmental samples[2]. A number of studies have highlighted limited abundance sensitivity as an issue impacting ^{129}I measurement by ICP-MS[15,21,24].

The internal standard used to correct for variations in instrument performance over the course of a run must be carefully considered for iodine. Previous studies have used In, Re, Cs or Te, however, there is no consensus as to which one is the most suitable, as stability in alkaline media and a high first ionisation energy are desirable properties, along with a similar mass to the analyte and not being present in the sample matrix[13,15,24,25,35,41,42,43,44,45,46,47].

Commercially available tandem ICP-MS/MS (Figure 1) has shown improved interference removal compared to alternative instrument configurations for several radionuclides, including ^{90}Sr[48], $^{135}Cs/^{137}Cs$[49] and ^{129}I[14,15]. Reviews of radionuclides measurable by ICP-MS/MS have been published elsewhere[50,51]. ICP-MS/MS consists of two quadrupole mass filters (termed Q1 and Q2) separated by a collision/ reaction cell (Figure 1). The quadrupole mass filter prior to the cell entrance (Q1) improves abundance sensitivity and therefore tailing removal compared to single quadrupole designs from ~10^{-7} to less than 10^{-10}. The first quadrupole mass filter also filters the ion beam by a single mass unit prior to the cell entrance, improving understanding of reactions in the cell compared to single quadrupole designs, as well as reducing or eliminating the formation of cell-based polyatomic interferences. Isobaric and polyatomic interferences can be removed using collision (e.g. H_2 and He) and/or reaction (e.g. O_2 and NH_3) gases to support or even replace offline chemical separation.

ICP-MS/MS has been effectively used for measurement of ^{129}I and $^{129}I/^{127}I$ isotopic ratios[14,15,16]. The additional quadrupole improved removal of ^{127}I tailing and in-cell polyatomics such as $^{97}Mo^{16}O_2$, whilst O_2 reaction gas reduced the signal from isobaric ^{129}Xe via a charge-transfer reaction. Additionally, when compared to a single quadrupole reaction cell instrument, the use of a negative voltage gap (termed

DOI: 10.1039/D3JA00045A

energy discrimination) between the cell and the second quadrupole (Q2) suppressed the ^{129}Xe signal using O_2 gas without significantly reducing the iodine signal. In a study by Matsueda et al., a combination of O_2 and CO_2 was used for ^{129}Xe and $^{127}I^{1}H_2$ removal, achieving a ratio of (m/z 129 background / ^{127}I of 4.6×10^{-10} [16]. The tandem ICP-MS/MS setup has been effectively used in the measurement of $^{129}I/^{127}I$ in rainwater, and Fukushima-contaminated soil samples following pyrohydrolysis and solvent extraction sample preparation.

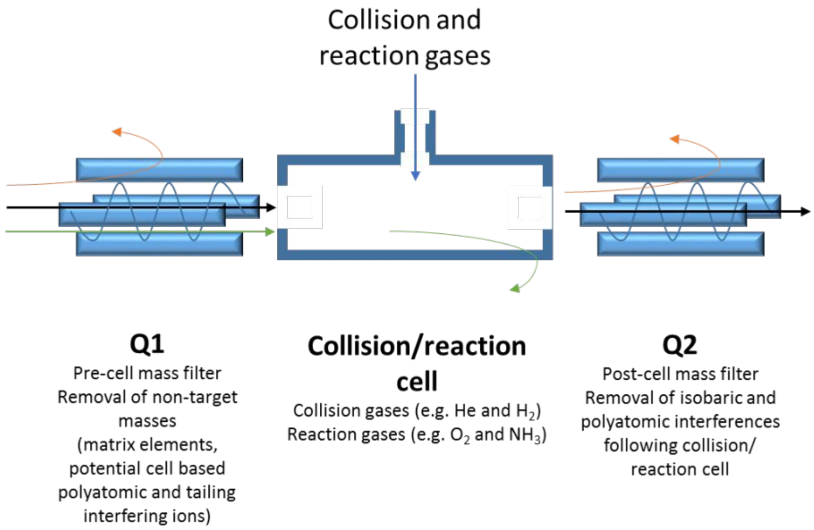

Figure 1. ICP-MS/MS layout and potential benefits of the tandem configuration.

This study presents a systematic assessment of the capability of ICP-MS/MS for routine ^{129}I measurement for nuclear decommissioning waste assay. As well as building on previous studies based on ICP-MS/MS, the use of matrix modification for improved sensitivity was investigated for ^{129}I for the first time. The study also evaluates a range of internal standards to assess their suitability. The optimised procedure was applied to a range of nuclear waste matrix simulants representative of decommissioning wastes. Following selective iodine extraction using thermal desorption, results were measured using both ICP-MS/MS and LSC.

2. Methodology

2.1 Reagents and Materials

Tetra methyl ammonium hydroxide pentahydrate (TMAH, ≥97%), glycerine (≥99.5%), sodium iodide (≥99%), ammonium iodide (≥99%), single element standard solutions of Te, In, Mo, Cd, Cs, Ce, Co, Li, Tl (10 mg g^{-1}) and Y (1 mg g^{-1}) were sourced from Sigma Aldrich, UK. Methanol (99.99%) was obtained from Fisher Scientific, UK. Iodine-129 standard solution (as NaI) (ISZ44) was obtained from Isotrak Amersham Laboratories, UK. Dilutions were prepared using deionised water (>18.2 MΩ·cm), produced from a Q-Pod Millipore System (Merck, UK).

2.2. Instrumentation

DOI: 10.1039/D3JA00045A

All ICP-MS measurements were performed using an Agilent 8800 ICP-MS/MS. The instrument is equipped with a collision-reaction cell (termed an Octopole Reaction System, ORS[3]) positioned between two quadrupole mass filters. A Scott double pass spray chamber, Micromist nebuliser, quartz torch and nickel sample and skimmer cones were used for all measurements. The instrument was fitted with four cell gas lines - dedicated H_2 and He lines, NH_3 in line 3 (for corrosive gases) and O_2 in line 4 (for non-corrosive gases). Ammonia was balanced in 90% He to protect the cell from corrosion, and when operating cell line 3, the He line was automatically run at a flow rate of 1 mL min^{-1}. High purity H_2, He, NH_3, O_2 and Ar were supplied by BOC (UK), with a purity of 99.9999% (N6.0). The instrument was tuned each day in single quadrupole (SQ) mode (only Q2 operating) with no cell gas using a 1 ng g^{-1} stable element standard mixture of Ce, Co, Li, Tl and Y in 0.3 M HNO_3. This procedure was intended to ensure criteria for sensitivity, measurement uncertainty, oxide and doubly charged ion formation and peak axes alignment were achieved. The instrument was then conditioned with deionised water for approximately 20 minutes to remove HNO_3, before transitioning to alkaline solution. In this study, all iodine samples were prepared in TMAH, as this was also used for selective extraction of ^{129}I from solid decommissioning matrices through a tube furnace procedure (see 2.3.6).

For method validation using simulated waste materials, extraction of ^{129}I was performed using a Raddec Pyrolyser Trio™ (a 3-zone tube furnace system that can accommodate 6 worktubes) configured with only glass components (i.e. no plastics). The catalyst zone was filled with crushed quartz to provide a non-reactive, tortuous path for off gases to transit and ensure oxidation of volatile organic species.

All LSC measurements were performed using a Wallac 1220 Quantulus liquid scintillation counter. A certified ^{129}I standard was counted in TMAH with Goldstar scintillation cocktail (Meridian Biotechnologies, UK) in polyethylene vials and the counting efficiency was determined. Subsequent samples were then prepared using the same ratio and concentration of TMAH to Goldstar and the counting efficiency was applied to each sample. The extent of quenching was monitored by comparing the external standard quench parameter (SQPE) for the ^{129}I standard, instrument blank and sample. All measurements were of comparable quench and therefore validated the counting efficiency. No colour quench was observed. The measurement window was set to provide the optimum efficiency-to-background ratio for ^{129}I measurement. Blank correction was applied to all measurements.

2.3 Experimental

2.3.1 Interference removal

Abundance sensitivity and hydride formation were assessed under both SQ and MS/MS modes with no cell gas, by introducing stable ^{127}I at concentrations ranging from 0.01 ng g^{-1} to 100 µg g^{-1} and monitoring m/z = 125, 126, 127, 128 and 129. The contribution of Xe isotopes was monitored at m/z = 128, 129 and 131. Stable iodine-based interferences were further investigated by increasing the ^{127}I

View Article Online
DOI: 10.1039/D3JA00045A

concentration in a solution containing a fixed activity of ^{129}I over a ^{129}I/^{127}I ratio ranging from 10^{-2} to 10^{-8} (representative of decommissioning samples) and measuring the change in signal at m/z = 129.

Polyatomic interference formation was assessed by introducing 0.001-10 µg g^{-1} of key elements that form polyatomic interferences (Mo, In, Cd and Y) and monitoring the signal at m/z = 129 in both SQ and MS/MS mode with no cell gas.

The effect of matrix composition on signal sensitivity was investigated by the impact of carbon content (from CO_2 liberated during sample combustion and subsequently co-trapped in TMAH as a carbamate) on sample introduction, signal stability and sensitivity on the ICP-MS/MS was investigated with CO_2 concentrations ranging from 0.001 g to 1 g.

The details of the iodine tube furnace extraction procedure is the focus of a separate study[51]. In this study, co-extraction of elements that can potentially form polyatomic interferences were assessed by testing the extraction / trapping efficiency of Y, Mo, Cd, In, Sn and Ba in 3 % TMAH and 0.6 M HNO_3. Sample measurement was performed in MS/MS mode with no cell gas.

2.3.2 *Sensitivity assessment*

Iodine sensitivity was initially assessed using a 10 ng g^{-1} stable ^{127}I solution prepared in 0.5 % TMAH. The sample was measured in SQ and MS/MS modes with no cell gas, as well as MS/MS mode with collision (H_2 and He) and reaction gases (NH_3 and O_2), using the auto tune parameters for each gas mode. Each gas flow rate was then varied to determine the optimal flow rate for iodine sensitivity and interference removal, focusing on suppression of ^{129}Xe. In NH_3 mode, a product ion scan was performed where Q1 was set to m/z = 127 and Q2 measured single mass units from m/z = 127 to m/z = 260 to determine if any iodine-based cell products were formed. In O_2 mode, the signal was measured both on m/z = 127 and 129 and on the shifted signals m/z+16 to potentially separate iodine and Xe through oxide formation. The lens, quadrupole and cell settings were also manually tuned to optimise for iodine sensitivity and Xe background suppression.

2.3.3 Matrix modification

The impact of a carbon-rich matrix on sensitivity was investigated using TMAH, glycerol and methanol as carbon sources. Stable ^{127}I standards from 0.001 ng g^{-1} to 25 ng g^{-1} and blanks were prepared in 0.5-3 % TMAH, and in 0-3 % methanol and glycerol at a fixed TMAH concentration of 0.5 %. The signals at m/z = 127 and m/z = 129 were monitored to assess the impact of varying sample matrix on the blank background signal on m/z = 129 and stable iodine background and sensitivity on m/z = 127.

2.3.4 Internal standard assessment

Indium and tellurium were evaluated as internal standards. The suitability was assessed on their similarity in mass and ionisation energy to ^{129}I, solubility in basic media, the potential to form polyatomic interferences, and the concentration in the samples being measured. Internal standards were

View Article Online
DOI: 10.1039/D3JA00045A

assessed for their effectiveness in correcting signal suppression arising from high matrix loading of stable ^{127}I (up to 10,000 µg g^{-1}) at ^{129}I activity concentrations of 6.4 mBq g^{-1} and 63.7 mBq g^{-1}, equivalent to 1.0 ng g^{-1} and 10.0 ng g^{-1}, respectively, in 3 % TMAH.

2.3.6 Measurement of decommissioning samples

Representative nuclear waste simulant samples, including graphite, ion exchange resins, silo liquors and $Mg(OH)_2$ based slurries and clinoptilolite were assessed. Each sample containing 0.5 g (clinoptilolite, graphite and ion exchange resin) or 1 g (other test materials) simulant was spiked with approximately 23.0 Bq (3.6 µg) ^{129}I, except for ion exchange resin that was spiked with 11.5 Bq (1.8 µg). Samples were combusted at 900 °C in a flow of air using a tube furnace and iodine was then trapped in 20 mL of 3 % TMAH. Iodine-129 activities were measured directly, and also following dilution by a factor of 10 and 100 to evaluate the measurement of ^{129}I at the target out-of-scope limit (0.01 Bq g^{-1}).The ICP-MS/MS was calibrated using ^{129}I standards ranging from 6.4×10^{-3} - 1.3 Bq g^{-1} (1 to 200 ng g^{-1}). Sub-samples of the trapping solution were also measured by LSC and values compared with those calculated by ICP-MS/MS.

3. Results and Discussions

3.1 Interference removal

Iodine-127 tailing removal is dependent on the abundance sensitivity of the instrument. Tailing was assessed at m/z = 126 and 125 i.e. m/z = -1 and m/z = -2, at increasing concentrations of ^{127}I, as low mass tailing is not affected by iodine hydride or dihydride formation. This approach assumes symmetrical tailing on the low mass and high mass side. Operating in MS/MS mode, the signal at both m/z = 125 and 126 was not elevated above background (<10 CPS). On the high mass side, the signal at m/z = 129 from ^{129}Xe was corrected based on the signal at m/z = 131 (^{131}Xe), so that the only significant contribution was from either ^{127}I tailing or $^{127}I^1H_2$. An increase in signal was observed at m/z = 129 at ^{127}I concentrations of 1 µg g^{-1} and above in Single Quad mode (Figure 2), equivalent to ~ 0.03 CPS per ng g^{-1}. Switching to MS/MS mode reduced this effect to < 0.001 CPS per ng g^{-1}. Assuming equal tailing on the low and high mass sides, the increase in signal most likely reflects $^{127}I^1H_2$ formation in the plasma.

View Article Online
DOI: 10.1039/D3JA00045A

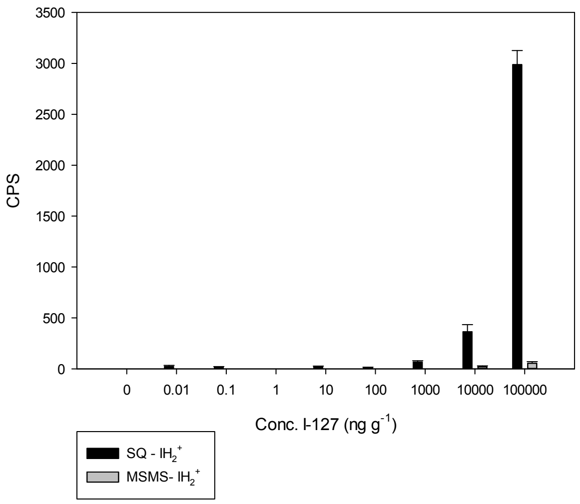

Figure 2. Signal on m/z = 129 with increasing concentrations of ^{127}I in SQ and MS/MS modes

Under no gas MS/MS mode, the ^{127}I sensitivity was ~20,000 CPS per ng g^{-1} with a background at m/z = 129 of ~2,000 CPS from isobaric ^{129}Xe (Table 2). Cell gases were introduced to assess the impact on the background at m/z = 129 and the iodine sensitivity. Using He, the ^{129}Xe background was reduced to 0 CPS when the flow rate reached 8 mL min^{-1}, but also reduced the ^{127}I signal to 300 CPS per ng g^{-1}. The same flow rate of H_2 reduced the background to ~600 CPS, with an ^{127}I sensitivity of ~6,500 CPS per ng g^{-1}. Ammonia at a flow rate of 3 mL min^{-1} removed the ^{129}Xe background, however, the iodine signal was reduced to <3 CPS per ng g^{-1}, and no significant cell products were formed from the product ion scan, suggesting NH_3 was not effective as a reaction gas.

Table 2. Iodine sensitivity and background at m/z = 129 for different cell gases in MS/MS mode

Cell gas	Flow rate (mL min^{-1})	^{127}I sensitivity (CPS per ng g^{-1})	^{129}Xe background (CPS)
No gas	-	20,000	2,000
H_2	8	6,500	600
He	8	300	<10
NH_3	3	<10	<10
O_2	0.5	15,000	60

In agreement with previous studies, the use of O_2 effectively reduced the ^{129}Xe signal at m/z = 129[13,14,15], with a flow rate of 0.5 mL min^{-1} reducing the signal at m/z = 129 by >97 % (~60 CPS) whilst retaining an ^{127}I sensitivity of ~15,000 CPS per ng g^{-1}. Rather than oxide formation, ^{129}Xe reduction is a result of a charge transfer reaction between O_2 and ^{129}Xe, with ^{129}Xe neutralisation preventing it from exiting the cell. To further minimise the contribution of the background, a baseline-subtraction can be applied,

View Article Online
DOI: 10.1039/D3JA00045A

which monitors m/z = 129 before and after a sample, and then subtracts the blank signal intensity. The long-term variation in background must be as well understood as possible for this to be applied, and an additional measurement uncertainty will be introduced.

Polyatomic interference formation was initially assessed by introducing solutions containing up to 100 µg mL^{-1} of Mo, In, Cd and Y. In SQ O_2 (0.5 mL min^{-1}) mode, a relative signal (129/signal on mass) of $<1.0\times10^{-9}$ was observed for both In and Y. However, both ^{113}Cd and ^{97}Mo showed a contribution on m/z = 129 with a relative signal of 10^{-4} associated with $^{113}Cd^{16}O$ and $^{97}Mo^{16}O_2$, respectively. When operating the instrument in MS/MS mode with O_2 reaction gas (0.5 mL min^{-1}), $^{113}Cd^{16}O$ formation was reduced to $<1.0\times10^{-9}$, suggesting the majority of $^{113}Cd^{16}O$ was formed in the cell rather than the plasma, which is overcome by removal of ^{113}Cd by setting Q1 to m/z=129. The formation of $^{97}Mo^{16}O_2$ was reduced by a factor of 10^2 in MS/MS O_2 compared to SQ O_2 mode (Figure 3), suggesting some formation of MoO_2 in the plasma, which passes through Q1. In SQ mode, Mo and plasma-formed MoO also pass through to the cell and react with O_2 to form MoO_2. Molybdenum concentrations of 0.5 µg mL^{-1} and above will interfere with the signal at m/z = 129 under MS/MS O_2 mode, whilst an increase in signal was observed at 0.001 µg g^{-1} in SQ O_2 mode (Figure 3). The use of MS/MS O_2 mode therefore increases the Mo concentration that can be tolerated, with offline chemical separation required if the concentration is above 0.5 µg mL^{-1}.

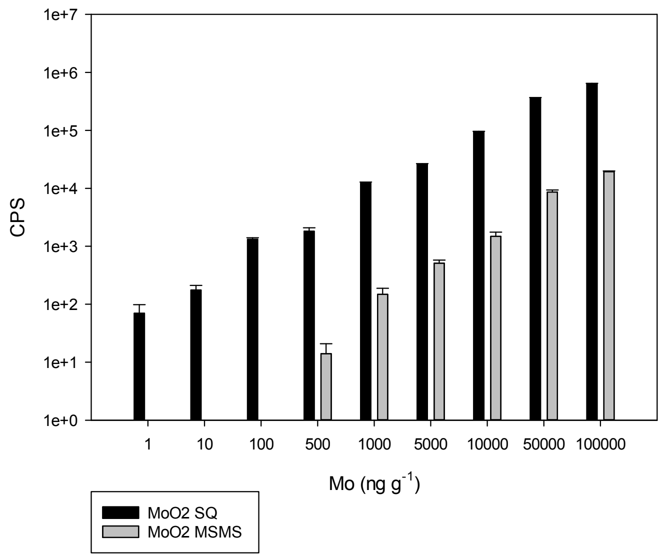

Figure 3.MoO_2^+ formation in SQ and MS/MS modes

Offline separation of polyatomic interferences was assessed by running a mixed solution containing 0.5 µg Mo, Cd, In, Y, Sn and Ba through the thermal desorption separation technique used for iodine extraction[51], with a 3 % TMAH trapping solution and 0.6 M HNO_3 trapping solution in sequence (Table 3). Of the elements tested, <1 % of Y, Cd and In were volatilised and trapped in the TMAH fraction. In the case of Mo, 1 % of the original Mo was measured in the TMAH fraction. Combined with the optimal ICP-MS/MS setup being able to tolerate 0.5 µg mL^{-1} Mo, this means starting Mo concentrations of 50 µg g^{-1} and above will result in an interference affecting ^{129}I measurement. The extraction technique therefore effectively separated potential polyatomic interferences, whilst achieving an average ^{129}I recovery of 90 % across a range of matrices. Sn and Ba were included as they can give rise potential isobaric interferences for In and Te internal standards, respectively. Barium was not co-extracted with the iodine with a recovery of <0.01 % in the TMAH fraction. This shows that the technique can tolerate a high Ba concentration with no significant impact on the internal standard measurement. However, Sn was found to volatilise with ~21 % trapped in the TMAH fraction meaning further consideration is required for samples rich in Sn if using In as an internal standard, due to potential interference from ^{115}Sn (0.34 % abundance).

Table 3. Recoveries of 1 µg g^{-1} solutions of ^{129}I interferences in TMAH (3 %) and HNO_3 (0.6 M) following tube furnace extraction

Element	Volatilisation through the tube furnace %	
	TMAH (3 %)	HNO_3 (0.6 M)
^{89}Y	0.0015	1.04
^{95}Mo	1.35	0.82
^{111}Cd	0.00076	0.01
^{115}In	0.22	0.02
^{118}Sn	21.1	0.73
^{137}Ba	0.0096	1.69

The thermal desorption separation technique used will decompose carbon-rich samples, releasing CO_2 which is co-trapped in TMAH as a carbamate. An assessment of the impact of carbamate concentration on plasma stability and dampening of the plasma due to an increased matrix loading was undertaken over a range of CO_2 concentrations (0.001 g to 1 g). No significant signal suppression was observed, with ^{129}I activity concentrations measured by ICP-MS/MS being between 93 % and 97 % of the expected values measured by LSC.

3.2 Sensitivity assessment

Increasing the O_2 flow rate up to 0.4 mL min^{-1} increased the ^{127}I sensitivity to a peak value of ~15,500 CPS per ng g^{-1}. The signal increase is a result of collisional focusing, which reduces the translational energy and concentrates the ion beam to the centre of the quadrupole mass filter. Above 0.4 mL min^{-1}, collisional energy dampening results in a reduced signal sensitivity[52]. Increasing the flow rate to 0.5 mL min^{-1} slightly reduced the iodine sensitivity to ~14,000 CPS per ng g^{-1}, but reduced the background signal at m/z = 129 (Figure 4), with an optimal 127/129 figure of merit (FoM) observed for an O_2 flow rate of 0.5 mL min^{-1}. At the maximum O_2 flow rate (1 mL min^{-1}) the analyte signal was suppressed by >65 % to ~4,000 CPS per ng g^{-1}, and whilst the background suppression at m/z = 129 was >99 % (~15 CPS remaining), the overall figure of merit was less favourable (Figure 4). The maximum $^{127}I^{16}O$ formation rate calculated was 9 % across the O_2 flow rate range compared to the on-mass signal, due to unfavourable thermodynamics (ΔH_r = +2.08), justifying on-mass measurement.

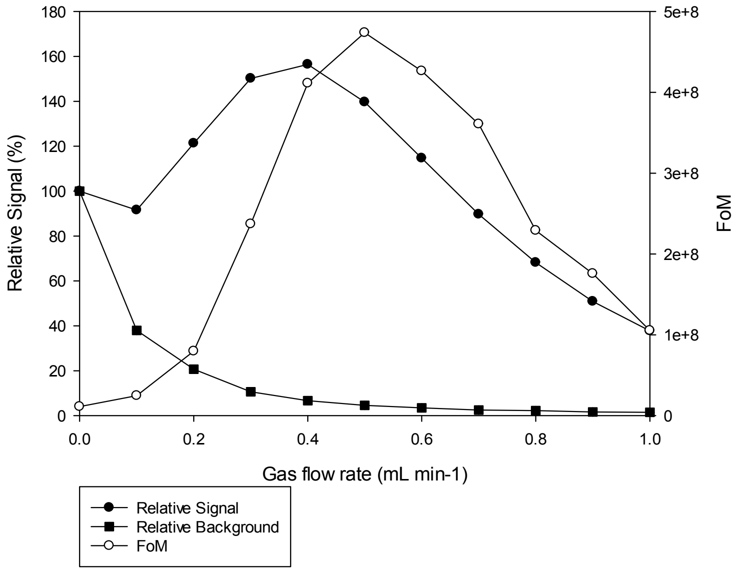

Figure 4. Variation in background signal, iodine sensitivity and figure of merit (FoM) with varying oxygen flow rates relative to MS/MS no gas mode.

Custom tuning of the lens, quadrupole and cell settings was investigated for potential improvement in the sensitivity and/or interference removal. The auto tune parameters for the majority of the lens and Q1 parameters were optimal. An improvement in sensitivity of ~20 % was achieved by shifting from a negative to a positive lens deflect voltage. This change improved the removal of plasma photons, metastable and neutral species and allowed the ion beam to maintain a robust focus[52].

The cell parameters were the most significant with regards to impact on sensitivity and interference removal. The octopole bias affects the energy of ions in the cell. In MS/MS O_2 mode (0.5 mL min^{-1}) at the auto tune value of -10 V, the instrument background from $^{129}Xe^+$ was ~500 CPS. Increasing the octopole bias to -5 V increased this value to ~600 CPS, with an improvement in iodine sensitivity from ~15,000 CPS to ~25,500 CPS per ng g^{-1}, doubling the signal to noise ratio and decreasing the $^{129}Xe/^{127}I$ ratio from 0.031 to 0.015. No further improvements were observed with changes in octopole bias. Xenon reacts >10^4 times faster with O_2 than iodine[21], allowing for a less negative octopole bias to be used to achieve a near complete charge transfer for Xe^+ with O_2 while also improving the iodine signal.

Kinetic energy discrimination (KED) controls cell-based interferences within the cell by attenuating them based on their size and/or energy[53]. This is especially useful for polyatomic interferences.

View Article Online
DOI: 10.1039/D3JA00045A

However, the slightly larger ionic radius and therefore collisional cross section of Xe (216 pm) compared to iodine (198 pm) means it is possible to use KED to improve Xe separation[54]. A negative KED value is required to account for the analyte energy loss when operating with a reaction gas. A value of -7 V gave the optimal signal to noise ratio, with the sensitivity reducing as the KED increased towards 0 V or reduced below -7 V.

3.3 Matrix Modification

An improvement in iodine sensitivity of ~60 % was achieved by increasing TMAH concentrations from 0.5 % to 3 %, compared to ~80 % improvement for the same concentration range of methanol and glycerol (Figure 5). The TMAH contained a 0.5 ng g^{-1} iodine impurity, increasing the background at m/z = 127 as the TMAH concentration increased. By comparison, the change in background at m/z = 127 with methanol and glycerol modification was proportional to the signal improvements associated with increased matrix modification, indicating that the signal increase resulted from enhancement of the signal from the trace iodine present in the original 0.5 % TMAH solution. No significant changes in background at m/z = 129 were observed under all matrix modifications for no gas and MS/MS O_2 modes, meaning the double charge transfer process is not occurring for Xe isotopes. The improved iodine sensitivity with no change in background interference on m/z = 129 further improved the figure of merit in MS/MS O_2 mode (0.5 mL min^{-1}) by an order of magnitude from 10^8 to 10^9.

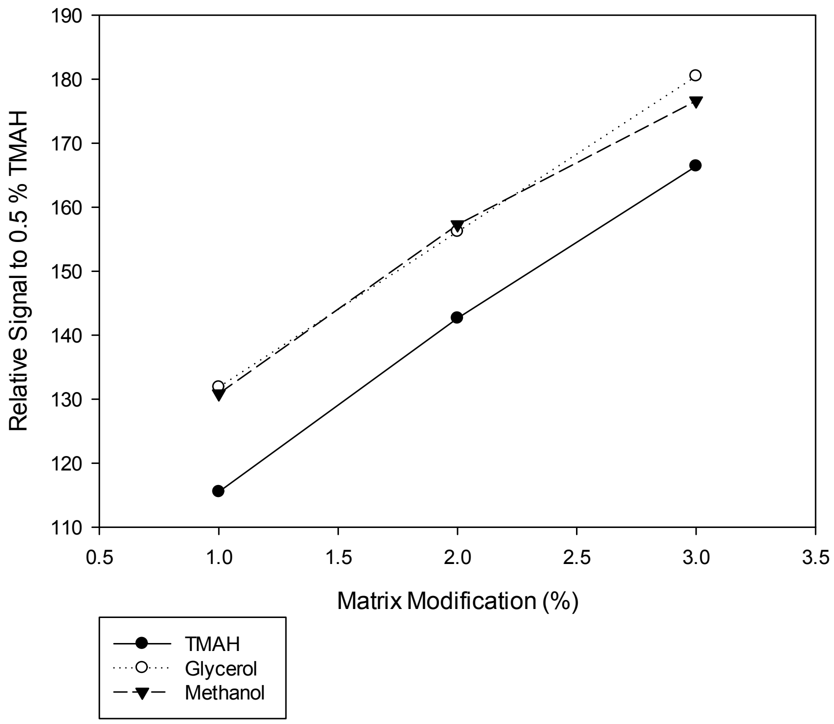

Figure 5: Impact of matrix modification on relative signal sensitivity compared to 0.5 % TMAH solution

View Article Online
DOI: 10.1039/D3JA00045A

The stable ^{127}I contamination with increased TMAH concentration has implications for $^{127}I/^{129}I$ ratio measurements, which could potentially be resolved using higher purity TMAH. Methanol matrix modification is favourable for isotopic ratio analysis because of its lack of stable ^{127}I contamination, and the ease of handling compared to more viscous glycerol. A maximum content of 3 % is recommended, as higher concentrations may result in an increase in plasma instability and higher measurement uncertainty.

3.3 Internal Standard

Using the optimised instrument setup described in sections 3.1-3.3, a solution containing 5 ng g^{-1} Te produced a signal of ~1×10^6 CPS in 3 % TMAH for ^{128}Te and ^{130}Te (31.74 % and 34.08 % abundance, respectively), with no measurable increase in background at m/z = 129 from tailing or hydride formation. However, the $^{127}I^1H^+$ formation rate of ~4×10^{-5} means concentrations of ^{127}I above 1 µg g^{-1} (expected in real samples) would contribute to the signal at m/z = 128, limiting the application of ^{128}Te. For ^{130}Te, the relatively low concentrations of ^{129}I tested (1 - 200 ng g^{-1} (0.0064 - 1.27 Bq g^{-1})) does not result in an overlap from tailing or polyatomic $^{129}I^1H^+$. Isobaric ^{130}Xe (4.07 % abundance) was suppressed to background levels (<10 CPS) through charge transfer with O_2. Isobaric ^{130}Ba (0.11 % abundance) was detected, but only after Ba concentrations exceeded ~10 µg g^{-1}, increasing the signal on m/z = 130 by ~10 % of the measured ^{130}Te signal (~1×10^6 CPS). In practice, the presence of sample-derived Ba in the purified fraction submitted for ICP-MS measurement will be minimised through the iodine thermal desorption extraction step, with <0.01 % trapped in 3 % TMAH. This would allow for a maximum tolerance of ~10 % Ba in the original sample. Any residual remaining Ba following the tube furnace extraction can be monitored at m/z = 137 (11.23 % abundance) and potentially corrected for.

Indium-115 has a similar mass to ^{129}I, and no contribution to m/z = 129 from polyatomic $^{115}In^{14}N^+$ was detected at concentrations up to 10 µg g^{-1}. However, the significantly lower first ionisation energy (5.79 eV compared to 10.45 eV for iodine) is a limitation, and isobaric ^{115}Sn may impact measurement, as despite the low isotopic abundance (0.34 %), ~21% Sn was volatilised through the tube furnace into the TMAH fraction (Table 4).

When comparing the total correction factor of In and Te across a range of matrix loading concentrations, the difference in performance of the internal standards is significant, with ^{130}Te able to correct for 100 % of the ^{129}I signal suppression compared to 77 % using ^{115}In (Figure 6). The difference in ionisation efficiency in the plasma at 7000 K between iodine (~10 %), Te (~40 %) and In (~98 %) means that changes in plasma energy during a run (e.g. due to high matrix loading or fluctuations in plasma gas flow rate) are more accurately reflected by Te compared to In (Table 4). The difference in ionisation potential is more significant with higher matrix loading as the majority of lower ionisation energy ions are still ionized.

View Article Online
DOI: 10.1039/D3JA00045A

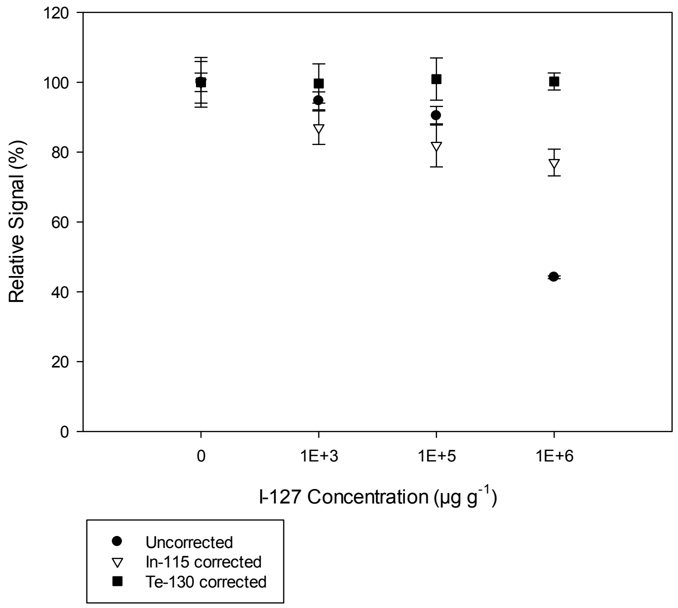

Figure 6: Comparison of internal Standard correction on 1 µg g^{-1} ^{129}I with increasing concentrations of ^{127}I

Table 4: Impact of plasma temperature (K) on ionisation potential for candidate ^{129}I internal standards (adapted from Jacobs 2015[55])

Element	Ionisation potential		
	6500 K	7000 K	7500 K
Iodine	3 %	10 %	29 %
Indium	95 %	98 %	99 %
Tellurium	15 %	40 %	66 %

The optimised instrument setup (Table 5) achieved an ^{129}I instrument detection limit (calculated as the equivalent concentration of three times the standard deviation of the blank) of 1.05×10^{-4} Bq g^{-1} (0.016 ng g^{-1}), when applied to ^{129}I standards. The instrument setups from previous studies were run as a comparison, which gave comparable detection limits in the case of Shikamori et al. 2012 (1.83×10^{-4}Bq g^{-1}, 0.029 ng g^{-1}) and Ohno et al., 2013 (1.96×10^{-4} Bq g^{-1}, 0.031 ng g^{-1}). The signal-to-noise ratio was also comparable across all three methods ($1.1\text{-}1.6\times10^{8}$). The instrument background (~40 CPS) was higher than in previous studies (2-4 CPS), which is likely due to the lower O_2 flow rate and/or matrix modification, however, this modification resulted in a sensitivity of 75,000 CPS for a 1 ng g^{-1} concentration, which is 4-6 times higher than previous studies.

Table 5: Optimised instrumental parameters for ^{129}I analysis

View Article Online
DOI: 10.1039/D3JA00045A

Instrument parameter	Value
Sample introduction media	0.5 % TMAH + 3 % methanol ($^{127}I/^{129}I$) Or 3 % TMAH (^{129}I)
Internal standard	5 ng g^{-1} Te (monitored at ^{130}Te)
Q1/Q2	129/129 (I)and 130/130 (Te)
RF power	1550 W
Scan mode	MS/MS
Plasma mode	Low Matrix
Extraction lens 1,2	0.0 V
Extraction lens 2	-190.0 V
Omega lens	8.2 V
Octopole Bias	-5.0 V
Energy discrimination	-7.0 V
O_2 gas flow rate	0.5 mL min^{-1}

3.4 Measurement of decommissioning samples

To assess the feasibility of ICP-MS/MS for routine measurement of ^{129}I for decommissioning samples, a range of nuclear waste simulants were analysed including $Mg(OH)_2$ sludge / liquor, ion exchange resin, clinoptilolite and graphite. Following tube furnace extraction, samples were split for measurement by both ICP-MS/MS and LSC, with the results compared against the reference values (Table 6). There was good agreement between LSC and ICP-MS/MS for all sample matrices measured.

The ^{129}I recovery through the tube furnace ranged from 84-99% across the samples tested, with the lowest values attributed to $Mg(OH)_2$ compared to other matrices (average recovery 86% for $Mg(OH)_2$) compared to 95% for other matrices. This is reflected in the lower values measured by LSC and ICP-MS/MS, however, the good agreement between ICP-MS/MS and LSC suggests that the low signal measured is not a result of matrix suppression.

There are no cases where the ICP-MS/MS results are significantly higher than for LSC, meaning any potential interference from tailing of polyatomic interferences are effectively removed using the optimal instrument setup. The ^{129}Xe counts in instrument blank samples ranged from 41-45 CPS, in good agreement with that achieved during method development. Xenon-130 (4.07 % abundance) was also monitored throughout the run, with count rates ranging from 5-55 CPS (average 23 CPS) across all samples measured, suggesting there is a contribution e.g. from ^{130}Ba. This compares to a ^{129}I sensitivity

DOI: 10.1039/D3JA00045A

of ~72,000 CPS for a 6.4 mBq g^{-1} (1 ng g^{-1}) solution, meaning minimal interference from isobaric ^{129}Xe whilst maintaining high sensitivity.

Table 6. Comparison of ICP-MS/MS and LSC measurement of ^{129}I in a range of decommissioning-relevant matrices. *20 mL 3% TMAH trapping solution was used for all samples.

Sample Type	Sample mass (g)*	LSC measured (Bq g^{-1} bubbler solution)	ICP-MS/MS measured (Bq g^{-1} bubbler solution)
Acid-washed sand	1	1.25 ± 0.02	1.27 ± 0.06
Silo liquor (saturated $Mg(OH)_2$ solution)	1	1.15 ± 0.02	1.18 ± 0.04
Sludge / slurry (50% $Mg(OH)_2$)	1	0.86 ± 0.01 0.94 ± 0.01	0.86 ± 0.05 0.93 ± 0.06
Ion exchange resin	0.5	0.58 ± 0.01 0.62 ± 0.01	0.57 ± 0.02 0.61 ± 0.02
Mineral (clinoptilolite)	0.5	1.20 ± 0.02 1.14 ± 0.02	1.23 ± 0.06 1.15 ± 0.05
Graphite	0.5	1.21 ± 0.02 1.09 ± 0.02	1.22 ± 0.06 1.09 ± 0.05

A 0.5% TMAH wash was applied after measurement of every sample. Whilst there was no evidence of cross-contamination impacting the results, the signal at m/z=129 was elevated in the wash following measurement of the higher activity samples. A longer wash and/or additional wash steps may need to be used in the case of higher activity samples. The ^{130}Te internal standard generally performed well, however, in ion exchange resin and graphite samples the count rate was 17-21 % higher than the value in the first sample run. These values were notably higher than the instrument drift measured over the course of the run (~10%), suggesting that there may be Te or potentially Ba contamination in the samples. Whilst Te is still believed to be the most suitable candidate for an internal standard and there is no evidence of interference with ^{129}I measurement in the samples tested, more detailed assessment of the Te content in decommissioning samples is required, as a higher internal standard concentration may be needed, providing there is no interference with ^{129}I.

The initial start-up, tuning and conditioning of the ICP-MS/MS takes approximately one hour, with a measurement time of ~3 minutes per sample, compared to a minimum of one hour per sample for LSC. The tube furnace technique used achieves a combination of extraction and separation of ^{129}I in a

View Article Online
DOI: 10.1039/D3JA00045A

single stage, which combined with ICP-MS/MS compares favourably to past procedures that require at least one additional separation stage prior to measurement[56]. A batch of six samples can be run at a single time through a single Pyrolyser-6 Trio tube furnace instrument, with a total procedural time on the order of three hours.

4. Conclusion

An optimised method has been developed for ^{129}I measurement in various nuclear waste assays by ICP-MS/MS. The instrumental design offers enhanced removal of isobaric, polyatomic and tailing interferences compared to alternative instrument designs. The first quadrupole mass filter removes elements that can potentially form cell-based polyatomics, most notably MoO_2. The use of O_2 as a reaction gas effectively reduces the isobaric ^{129}Xe interference by >97 %, whilst the additional mass filter also improves removal of stable ^{127}I tailing and polyatomic interferences, most notably MoO_2. The use of matrix modification in the form of an increased TMAH concentration allows for an improved signal sensitivity to compensate for the high first ionisation energy of iodine, improving the overall signal stability and signal-to-noise ratio. Tellurium (^{130}Te) was determined to be the most suitable internal standard for correcting for instrument drift and signal suppression associated with the high matrix loading of ^{127}I.

Five different solids and one aqueous sample were measured by ICP-MS/MS, with results showing good agreement with LSC. Iodine was extracted from solid samples by thermal desorption using a Pyrolyser tube furnace and extracted in 3% TMAH, before being spiked with an internal standard and then measured without additional sample preparation. An instrument detection limit of 1.05×10^{-4} Bq g^{-1} (0.016 ng g^{-1}) was calculated for ^{129}I, which is two orders of magnitude below the out-of-scope limit, providing a means for characterisation of nuclear waste materials with minimal procedural stages prior to measurement. The increasing number of nuclear facilities reaching a stage of decommissioning means a high throughput technique that can cope with a complex range of matrices makes this technique highly beneficial and offers a means of reducing time and cost of analysis and hence decommissioning overall.

5. References

1. NDA., 2019. 'Business Plan, 1 April 2019 to 31 March 2022', Publication number: SG/2019/48, *Nuclear Decommisoning Authority (NDA)* https://www.gov.uk/government/publications/nuclear-provision-explaining-the-cost-of-cleaning-up-britains-nuclear-legacy/nuclear-provision-explaining-the-cost-of-cleaning-up-britains-nuclear-legacy
2. X. Hou, V. Hansen, A. Aldahan, G. Possnert, O.C. Lind, and G. Lujaniene, *Anal. Chim. Acta.,* 2009, **632**, 181-196
3. H. Hijazi, 2017, FRNC-TH—10337, https://inis.iaea.org/search/searchsinglerecord.aspx?recordsFor=SingleRecord&RN=49107658

DOI: 10.1039/D3JA00045A

4. L. Devell, and K. Johansson, 1994, SKI Report 94:29 NEA/CSNI/R(94)28, Nyköping, Sweden
5. W.H. Hocking, R.A. Verrall, and I.J. Muir, J. *Nucl. Mat.*, 2001, **294**, 45-52
6. M. Honda, H. Matsuzaki, Y. Miyake, Y. Maejima, T. Yamagata, and H. Nagai, *J. Environ. Radioactiv.,* 2015, **146**, 35-43.
7. FEPC & JAEA, 2007, *Japan Atomic Energy Agency, The Federation of Electric Power Companies of Japan*. https://jopss.jaea.go.jp/pdfdata/JAEA-Review-2007-010.pdf
8. K. Umadevi, and D. Mandal, *J. Environ. Radioactiv.*, 2021, **234**,106623
9. A. Dyer, J. Hriljac, N. Evans, I. Stokes, P. Rand, S. Kellet, R. Harjula, T. Moller, Z. Maher, R. Heatlie-Branson, J. Austin, S. Williamson-Owens, M. Higgins-Bos, K. Smith, L. O'Brian, N. Smith, and N. Bryan, *J. Radioanal. Nucl. Chem.*, 2018, **318(3)**, 2473-2491.
10. IAEA, Safety Standards Safety Guide No. RS-G-1.7. Application of the Concepts of Exclusion, Exemption and Clearance, https://www-pub.iaea.org/mtcd/publications/pdf/pub1202_web.pdf
11. B.G. Fritz, and G.W. Patton, *J. Environ. Radioactiv.,* 2006, **86(1)**, 64-77.
12. T. Suzuki, S. Otosaka, J. Kuwabara, H. Kawamura, and T. Kobayashi, *Biogeosciences Discussions,* 2012, **10**, 1401-1419.
13. G. Yang, H. Tazoe, and M. Yamada, *Anal. Chim. Acta*, 2018, **1008**, 66-73.
14. Y. Shikamori, K. Nakano, N. Sugiyama and S. Kakuta, Publication number: 5991-1708EN, *Agilent Technologies, Inc. 2012, Technical Note*, 2012
15. T. Ohno, Y. Muramatsu, Y. Shikamori, C. Toyama, N. Okabe, and H. Matsuzaki, *J. Anal. Atom. Spectrom.,* 2013, **28**, 1283-1287
16. M. Matsueda, J. Aoki, K. Koarai, M. Terashima, and Y. Takagi, *Anal. Sci.*, 2022, **38**, 1371-1376
17. L. Zhang, X. Hou, T. Zhang, M. Fang, H. Kim, H. Jiang, N. Chen, and Q. Liu, *Anal. Chem.,* 2022, **94**, 9835-9843
18. J.A. Suárez, A.G. Espartero, and M. Rodríguez, *Nuclear Instruments and Methods in Physics Research, Section A: Accelerators, Spectrometers, Detectors and Associated Equipment,* 1996, **369(2-3)**, 407-410.
19. A. Zulauf, S. Happel, M.B. Mokil, A. Bombard, and H. Jungclas, *J. Radioanal. Nucl. Chem.*, 2010, **286**, 539-546.
20. A. Schmidt, C. Schnabel, J. Handl, D. Jakob, R. Michel, H.A. Synal, J.M. Lopez, and M. Suter, *Science Total Environment,* 1998, **223**, 131-156
21. A.V. Izmer, S.F. Boulyga, and J.S. Becker, *J. Anal. Atom. Spectrom.,* 2003, **18(11)**, 1339-1345.
22. Y. Miyake, H. Matsuzaki, T. Fujiwara, T. Saito, T. Yamagata, M. Honda, Y. Muramatsu, *Geochemical Journal*, 2012, **46**, 327-333
23. Y. Muramatsu, S. Yoshida, U. Fehn, S. Amachi, and Y. Ohmomo, *J. Environ. Radioactiv.,* 2004, **74**, 221-232.
24. S.K. Sahoo, Y. Muramatsu, S. Yoshida, H. Matsuaki, and W. Rühm, *Journal of Radiation Research, Volume*, 2009, **50(4)**, 325-332.
25. S. Szidat, A. Schmidt, J. Handl, D. Jakob, W. Botsch, R. Michel, H.A. Synal, C. Schnabel, M. Suter, J.M. Lópe-Gutiérrez, W. Städe, *Nuclear Instruments and Methods in Physics Research Section B: Beam Interactions with Materials and Atoms,* 2000, **172**, 699-710
26. C.F. Brown, K.N. Geiszler, and M.J. Lindberg, *Applied Geochemistry,* 2007, **22(3)**, 648-655.
27. J.S. Becker, and H-J Dietze, *J. Anal. Atom. Spectrom.,* 1997, **12**, 881-889.
28. K. Nakano, Y. Shikamori, N. Sugiyama, and S. Kakuta, *Agilent Application Note*, 2011, https://www.agilent.com/Library/applications/5990-8171EN_AppNote_7700x_Ultratrace_Iodine.pdf
29. I.W. Croudace, B.C. Russell, and P.E. Warwick, 2017, *J. Anal. Atom. Spectrom.,* 2017, **32**, 494-526

30. D. Beals, and D. Hayes, *Science of the Total Environment*, 1995, **173-174**, 101-115.
31. G. Kerl, J. Sabine Becker, J. Hans-Joachim Dietze, and W. Dannecker, *J. Anal.. Atom. Spectrom.,* 1996, 11, 723-726
32. D. Lariviere, V.F. Taylor, R.D. Evans, and R.J. Cornett, *Spectrochemica Acta Part B: Atomic Spectroscopy,* 2006, **61**, 877-904
33. X. Hou, and P. Roos, *Anal. Chima. Acta.,* 2008, **608 (2)**, 105-139
34. L. Bing, M. Xinrong, H. Lirong, and Y. Hongxia, *Geostandards and Geoanalytical Research*, 2007, **28 (2)**, 317-323
35. J. Zheng, H. Takata, K. Tagami, T. Aono, K. Fujita, S. Uchida, *Microchemical Journal,* 2012, **100(1)**, 42-47.
36. H.J. Reid, A.A. Bashammakh, P.S. Goodall, M.R. Landon, C. O'Connor, and B.L. Sharp, *Talanta,* 2008, **75(1)**, 189-197.
37. T.I. Todorov, and P.J. Gray, *Food Additives and Contaminants - Part A Chemistry, Analysis, Control, Exposure and Risk Assessment,* 2016, **33(2)**, 282-290.
38. A. Jerše, R.Raćimović, N.K. Maršić, M. Germ, H. Šircelj, and V. Stibilj, *Microchemical Journal,* 2018, **137**, 355-362.
39. G. Grindlay, J. Mora, M. De Loos-Vollebregt, and F. Vanhaecke, *Spectrochim. Acta. Part B Atomic Spectroscopy,* 2013, **86**, 42-49.
40. P. Bienvenu, E. Brochard, E. Excoffier, and M. Piccione, *Canadian Journal of Analyical Sciences and Sprectroscopy*, 2004, **49**, 423-428.
41. Ž Ežerinskis, A. Spolaor, T. Kirchgeorg, G. Cozzi, P. Vallelonga, H.A. Kjær, J. Šapolaitė, C. Barbante, and R. Kruteikienė, *J. Anal. Atom. Spectrom.,* 2014, **29(10)**, 1827-1834.
42. J. Lehto, T. Räty, X. Hou, J. Paatero, A. Aldahan, G. Possnert, J. Flinkman, and H. Kankaanpää, *Science of the Total Environment,* 2012, **419**, 60-67.
43. H. Fujiwara, K. Kawabata, J. Suzuki, and O. Shikino, *J. Anal. Atom. Spectrom.,* 2011, **26(12)**, 2528-2533.
44. J.A. Gomez-Guzman, S.M. Enamorado-Baez, A.R. Pinto-Gomez, and J.M. Abril-Hernandez, *Int. J. Mass. Spectrom.,* 2011, **303**, 103-108
45. V. Hansen, P. Roos, A. Aldahan, X. Hou, and G. Possnert, *J. Environ. Radioactiv.,* 2011, **102(12)**, 1096-1104.
46. X. Hou, P.P. Povinec, L. Zhang, K. Shi, D. Biddulph, C.C. Chang, Y. Fan, R. Golser, Y. Hou, M. Ješkovský, A.J.T. Jull, Q. Liu, M. Lou, P. Steier, and W. Zhou, *Environ. Sci. Technol.,* 2013, **47(7)**, 3091-3098.
47. J. Qiao, V. Hansen, X. Hou, A. Aldahan, and G. Possnert, 2012., *Appl. Radiat. Isotopes*, 2012, **70(8)**, 1698-1708.
48. B. Russell, M. García-Miranda, and P. Ivanov, *Appl. Radiat. Isotopes,* 2017, **126**, 35-39.
49. J. Zheng, K. Tagami, W. Bu, S. Uchida, Y. Watanabe, Y. Kubota, S. Fuma, and S. Ihara, *Environ. Sci. Technol.,* 2014, **48(10)**, 5433-5438.
50. W. Bu, Y. Ni, G. Steinhouser, W. Zheng, J. Zheng, N. Furuta, *J. Anal. Atom. Spectrom.,* 2018, **33**, 519-546.
51. P.E. Warwick, D. Reading, 2022, In preparation
52. S.D. Tanner, V.I. Baranov, and D.R. Bandura*, Spectrochimica Acta Part B, Atomic Spectroscopy*, 2002, **57**, 1361-1452
53. N.I. Rousis, I.N. Pasias, and N.S. Thomaidis, *Analytical Methods,* 2014, **6(15)**, 5899-5908.
54. N. Yamada, *Spectrochimica Acta Part B: Atomic Spectroscopy*, 2015, **110**, 31-44, https://lib.dr.iastate.edu/etd/14814
55. J.L. Jacobs, *Iowa State University Graduate Theses and Dissertations*, 2015, 14814,
56. F. Yiou, G. Raisbeck, and H. Imbaud, *Nuclear Instruments and Methods in Physics Research Section B: Beam Interactions with Materials and Atoms,* 2004, **223-224**, 412-415.